# Supporting Information

# Synergism of tiny Ni clusters and Pt nanoparticles promoting efficient and stable electrocatalytic methanol oxidation and hydrogen evolution by water electrolysis

Jie Huang [1, a, b], Ming Tian [1, d], Liang Tong [1, a], Lihua Zhu [1, a, *], Lingling Li [a], Xianping Liao [c], Qingsheng Gao [c], Weizhen Wang [d], Zhiqing Yang [d], Tongxiang Liang [b], Hengqiang Ye [d]

[a] Jiangxi Provincial Key Laboratory of Functional Molecular Materials Chemistry, College of Chemistry and Chemical engineering, Jiangxi University of Science and Technology, Ganzhou 341000, Jiang Xi, China

[b] College of Rare Earth, Jiangxi University of Science and Technology, Ganzhou 341000, Jiang Xi, China

[c] College of Chemistry and Materials Science, and Guangdong Provincial Key Laboratory of Functional Supramolecular Coordination Materials and Applications, Jinan University, Guangzhou 510632, China

[d] Ji Hua Laboratory, Foshan 528200, China.

Corresponding Author: zhulihua@jxust.edu.cn (Lihua Zhu)

[1] These authors contributed equally to this work.

## 1. Experimental Section

### *1.1. Catalyst Preparation*

Ni-TCPP was synthesized according to the previously reported method [1]. To refluxed propionic acid (100 mL) in a 500-mL three necked flask were added pyrrole (3.0 g, 0.043 mol) and methyl p-formylbenzoate (6.9 g, 0.042 mol), and the solution was refluxed for 12 h in darkness. After the reaction mixture was cooled to room temperature, crystals were collected by suction-filtration to afford purple crystals (5,10,15,20-Tetrakis(4-methoxycarbonylphenyl)porphyrin (TPPCOOMe)).

A solution of TPPCOOMe (0.854 g, 1.0 mmol) and $NiCl_2 \cdot 6H_2O$ (3.1 g, 12.8 mmol) in 100 mL of DMF was refluxed for 6 h. After the mixture was cooled to room temperature, 150 mL of $H_2O$ was added. The resultant precipitate was filtered and washed with 50 mL of $H_2O$ for two times. The obtained solid was dissolved in $CHCl_3$, followed by washing three times with 1 M HCl and twice with water. The organic layer was dried over anhydrous magnesium sulfate and evaporated to afford quantitative crimson crystals ([5,10,15,20-Tetrakis(4-methoxycarbonylphenyl)porphyrinato]-Ni(II)).

The obtained ester (0.75 g) was stirred in THF (25 mL) and MeOH (25 mL) mixed solvent, to which a solution of KOH (2.63 g, 46.95 mmol) in $H_2O$ (25 mL) was introduced. This mixture was refluxed for 12 h. After cooling down to room temperature, THF and MeOH were evaporated. Additional water was added to the resulting water phase and the mixture was heated until the solid was fully dissolved, then the homogeneous solution was acidified with 1.0 M HCl until no further precipitate was detected. The crimson solid was collected by filtration, washed with water and dried in vacuum (Ni-TCPP).

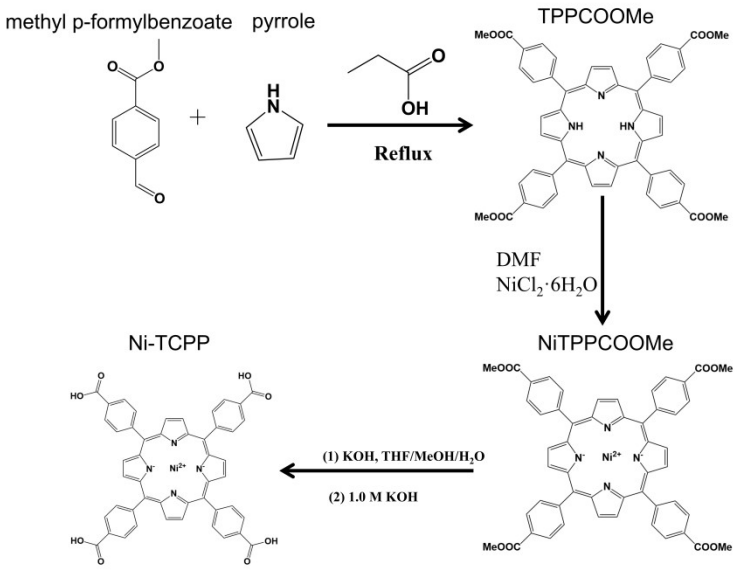


**Scheme S1.** Synthesis strategy for Ni-TCPP ligands.

*1.2. Structural characterization*

The phase characteristics of the samples were examined using SMART APEX II (Cu *Ka* radiation, λ = 1.54 Å, 40 kV, 30 mA). XPS spectra of the catalysts were recorded on PHI 5000 VersaProbe III. The particle size distribution and morphologies of the catalysts were determined using a TECNAI F30 transmission electron microscope (300 kV). We observed the atomic-level structure and elemental distribution of atoms using aberration-corrected microscope examinations (Titan G2 60-300). To further evaluate the performance of the catalyst, the metal loadings in the samples were determined by ICP-OES.

*1.3. Performance measurements*

A conventional three-electrode system (reference electrode-saturated calomel electrode, counter electrode-Pt sheet, and working electrode-catalyst-loaded glassy carbon electrode (MOR)/carbon paper (HER) was used for both MOR and HER. The electrochemical tests were all performed at room temperature using a CHI760E

electrochemical workstation in an $N_2$-saturated electrolyte. To convert the SCE potential to the reversible hydrogen electrode (RHE) potential, we used the following equation:

$$E_{RHE} = E_{SCE} + 0.0591\ V * pH + 0.02415\ V$$

where 0.2415 V was the potential difference of SCE with respect to the standard hydrogen electrode (SHE) and the pH of the experimental solution was 14 (experiments under alkaline conditions).

In the HER test, 2.0 mg of catalyst was homogeneously mixed with 0.4 mL of isopropanol and 0.1 mL of ultrapure water. The mixture was dripped evenly onto the surface of the carbon paper, dried and added to a 5% Nafion solution. The catalyst loading on the carbon paper was 2.0 mg $cm^{-2}$. The potential was set to -0.867 V~ -0.669 V (vs SCE) test CV curve, activated the catalyst, and set the sweep speeds to 0.01, 0.02, 0.04, 0.06, 0.08, and 0.10 V $s^{-1}$. Potentials were set -1.669 V to -1.069 V (vs SCE), and a sweep rate of 0.005 V $s^{-1}$ was used for the linear sweep voltammetry (LSV). Electrochemical Impedance Spectroscopy (EIS) measurements were conducted over a frequency range from 0.01 Hz to 100 kHz. Moreover, two typical methods were both carried out to appraise the stability of the catalysts. Fig. 3d, f were the continuous cyclic voltammetry, which was performed for 20000 cycles (sweep rate of 50 mV $s^{-1}$, 200 mV $s^{-1}$) from 0 V to -0.6 V (vs. RHE) and the other method was the chronoamperometry (CP) at 100 mA $cm^{-2}$ for 230 h.

Calculation of the specific surface area of Pt (electrochemical active area) in $Pt_{10}$/Ni-$ZrO_2$-NC = (238.9-120.6)/0.04 = 2957.5 $cm^2$. (238.9 mF $cm^{-2}$ and 120.6 mF $cm^{-2}$ were the $C_{dL}$ of $Pt_{10}$/Ni-$ZrO_2$-NC and Ni-$ZrO_2$-NC, respectively; the difference of [$C_{dL}$_$Pt_{10}$/Ni-$ZrO_2$-NC - CdL_Ni-$ZrO_2$-NC] represents the contribution of Pt to ECSA, the Cs of carbon-based materials = 0.04 mF $cm^{-2}$)

$$\text{Specific Activities} = \frac{j}{ECSA}$$

$$\text{Mass Activities} = \frac{j}{M_{Pt}}$$

$M_{Pt}$ was the actual Pt loading of the catalyst on the carbon paper surface, as calculated by ICP-OES.

For the MOR test: 2.0 mg of catalyst was mixed with 0.8 mL of isopropanol and 0.2 mL of ultrapure water. Subsequently, 10 μL of the catalyst mixture was added dropwise in two portions to the glassy carbon electrode. After the catalyst had dried, 10 μL of 0.25% Nafion solution was added dropwise. Then, 48 mL of a 1 M KOH solution was bubbled with nitrogen for 30 minutes, connected to an electrical circuit, and activated by cyclingat -1.069 V to 0.131 V (vs SCE) at 0.05 V/s for 80 cycles, followed by 5 more cycles at the same scan rate. The CV scan was then continued in 1.0 M KOH+1.0 M $CH_3OH$. The stability of the electrocatalytic oxidation of methanol was tested by conducting a 10000 s Chronoamperometry (CA) with a constant potential set at -0.250 V (vs. SCE), to monitor changes in current.

In the CO-stripping test, the working electrode was the same as that of the MOR. CO gas was continuously passed into a 1.0 M KOH solution at 0.109 V (vs. RHE) for 50 min to achieve maximum adsorption of CO at Pt. Then the bubbling with $N_2$ was continued at the same voltage for 10 min to exclude the residual CO in the solution, and the CV test was carried out in the potential interval of 0 ~ 1.25 V (vs. RHE) at a sweep rate of 0.05 V $s^{-1}$ until the characteristic peaks of CO did not appear.

We calculated the electrochemical specific surface area (ECSA, $m^2$ $g_{Pt}^{-1}$) based on Pd loadings measured by ICP-OES and the CO-stripping experiments. The calculations were performed as follows:

$$ECSA = \frac{Q}{M * 0.42}$$

$$Q = I * t = \frac{\int IdE}{v}$$

where M was the mass of Pt (mg) on the electrode, 0.42 mC $cm^{-2}$ was the charge consumed during electrooxidation of a CO monolayer, Q was the total charge (C) used for CO electrooxidation, v was the scanning rate (0.05 V $s^{-1}$), and $\int IdE$ was the

integrated area of the cyclic voltammetry curve of CO-stripping corrected for the double layer current.

Calculations of the ECSA of the samples were provided as follows：

The ECSA of Pt/C-JM catalyst：

$$ECSA_{electrode} = \frac{Q}{M * 0.42}$$

The calculation of mass activity was the same as the calculation of activity for HER as described above.

Two-electrode flow cell stability measurements for the [MOR||HER]: The cathode is prepared in the same way as the HER test, but requires 5.0 mg of catalyst. The anode needs to take 100.0 mg of catalyst dispersed in 3 mL of isopropanol aqueous solution, add 0.4 mL of 5% Nafion solution, evenly disperse ultrasonication for 30 min, add 10 carbon pads (0.5*0.5*0.5 $cm^3$) to the catalyst ink, absorb the fullness of the catalyst ink, take out the carbon pad, wait for the catalyst on the catalyst pad to dry, and then evenly fall the remaining catalyst on the carbon pad. During the test, both poles were simultaneously energized with $N_2$-saturated 1.0 M KOH solution, and the catalyst performance was tested using linear sweep voltammetry at 0.05 V/s. After the data were stabilized. The catalyst performance was further tested at the anode by adding an $N_2$ saturated 1.0 M KOH solution containing 1.0 M methanol to the anode. The stability of Two-electrode flow cell stability measurements was tested using the CA method (Cell voltage of 2.700 V).

The Operando Raman spectra of the samples were measured using a Horiba HR-800 Raman microspectrometer with an electrochemical workstation (CHI 660E). 1×1 $cm^2$ carbon paper-loaded catalyst (2.0 mg $cm^{-2}$) was used as the working electrode, a saturated calomel electrode as the reference electrode, and a graphite rod as the counter electrode in 1.0 M KOH solution. Raman spectra at different potentials were obtained and a 532 nm laser as the excitation light source.

**Table S1.** Pt and Ni loading in all catalysts prepared.

| Catalyst | Metal Ni (wt%) | Metal Pt (wt%) |
|---|---|---|
| Ni-$ZrO_2$-NC | 1.38 | |
| $Pt_1$/Ni-$ZrO_2$-NC | 1.35 | 1.03 |
| $Pt_{2.5}$/Ni-$ZrO_2$-NC | 1.33 | 2.38 |
| $Pt_5$/Ni-$ZrO_2$-NC | 1.31 | 4.68 |
| $Pt_{10}$/Ni-$ZrO_2$-NC | 1.28 | 9.27 |
| $Pt_{10}$/$ZrO_2$-NC | | 9.85 |

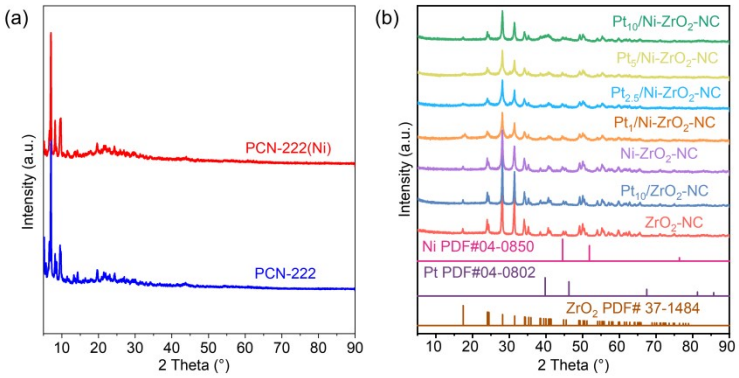


**Fig. S1.** (a) XRD patterns of PCN-222 and PCN-22(Ni), (b) XRD patterns of PCN-222 and PCN-22(Ni) after high-temperature carbonization and being loaded with Pt.

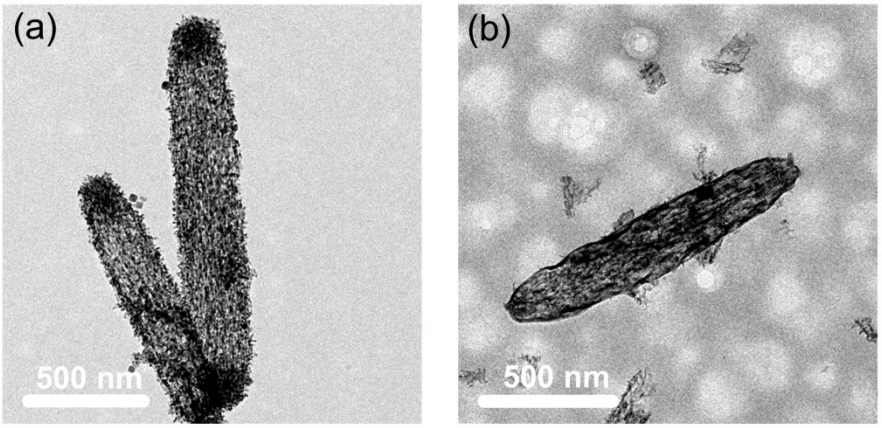


**Fig. S2.** TEM images of Ni-$ZrO_2$-NC and $ZrO_2$-NC.

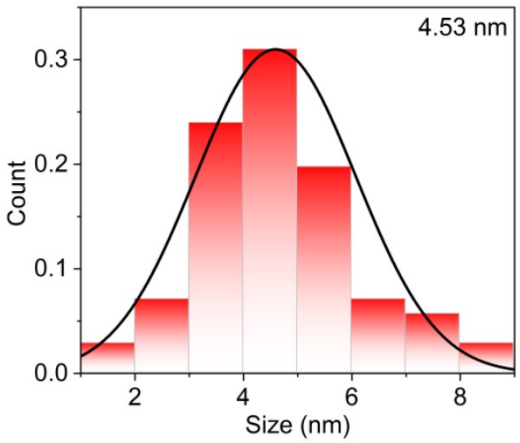


**Fig. S3.** Particle size distribution of $Pt_{10}$/Ni-$ZrO_2$-NC.

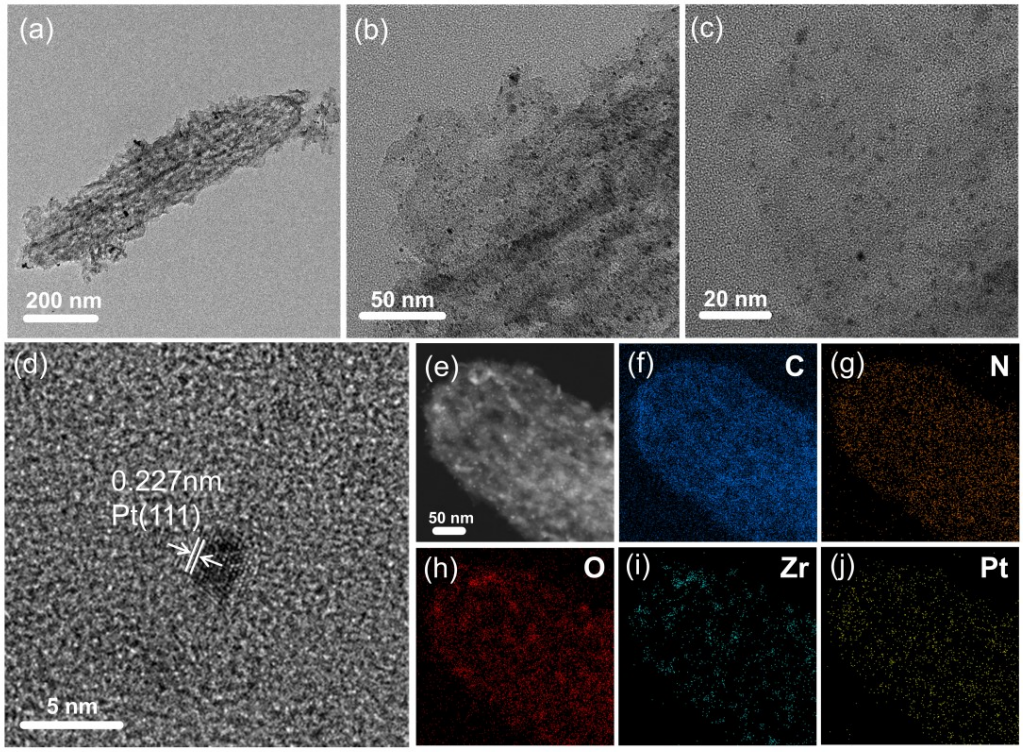


**Fig. S4.** (a-c) TEM; (d) HRTEM; (e) STEM image and STEM-EDX elemental maps of $Pt_{10}$/$ZrO_2$-NC-(f) C (biue), (g) N (orange), (h) O (red), (i) Zr (cyan), (j) Ni (green), (k) Pt (yellow).

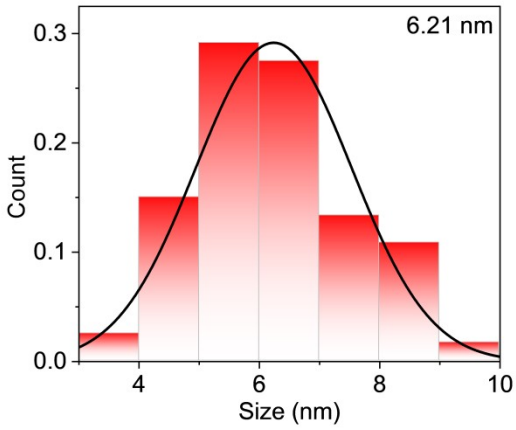


**Fig. S5.** Particle size distribution of $Pt_{10}/ZrO_2$-NC.

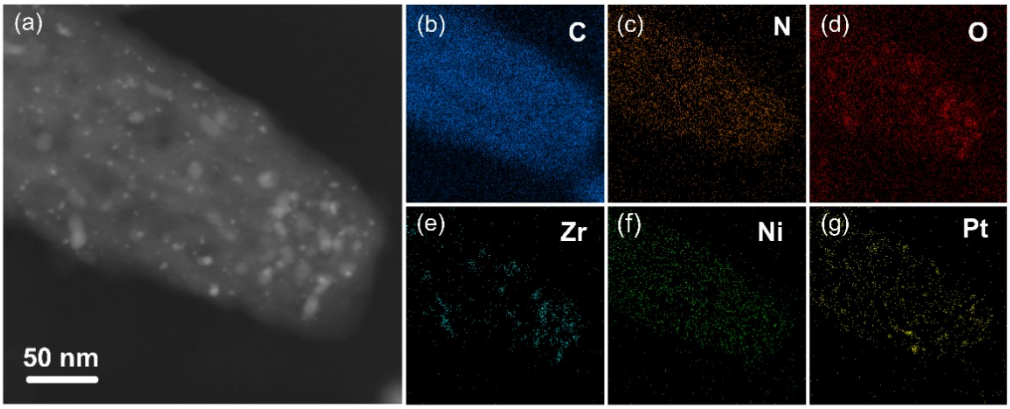


**Fig. S6.** (a) STEM image and STEM EDX elemental maps of $Pt_{10}$/Ni-$ZrO_2$-NC-(b) C (blue), (c) N (orange), (d) O (red), (e) Zr (cyan), (f) Ni (green), (g) Pt (yellow).

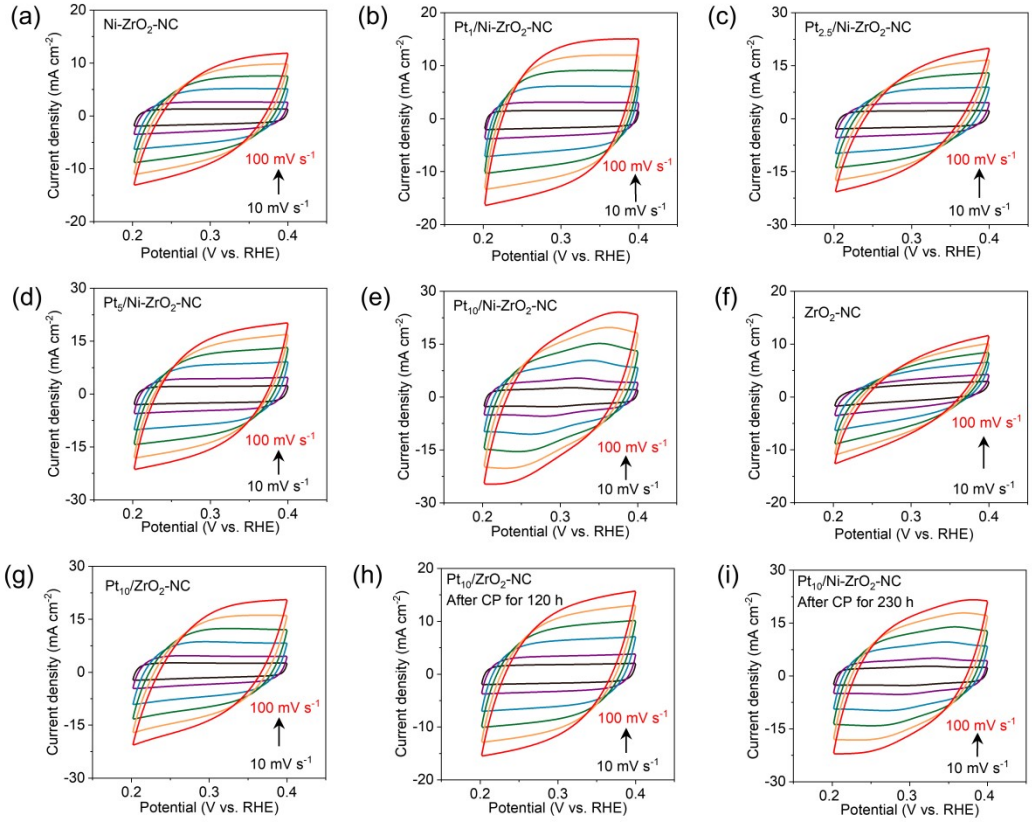


**Fig. S7.** CV curves of the catalysts.

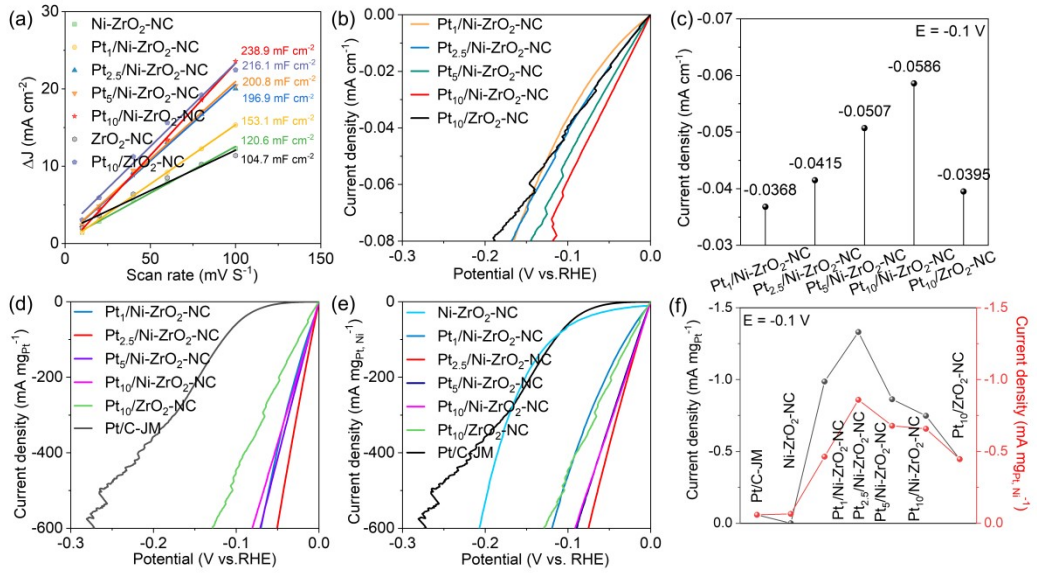


**Fig. S8.** (a) Linear fitting of the capacitive current versus the CV scanning rate; (b) ECSA normalization for all the as-prepared catalysts; (c) specific activities; (d) mass normalization of all prepared catalysts (for Pt loading); (e) mass normalization of all prepared catalysts (for Pt and Ni loading); (f) mass activities.

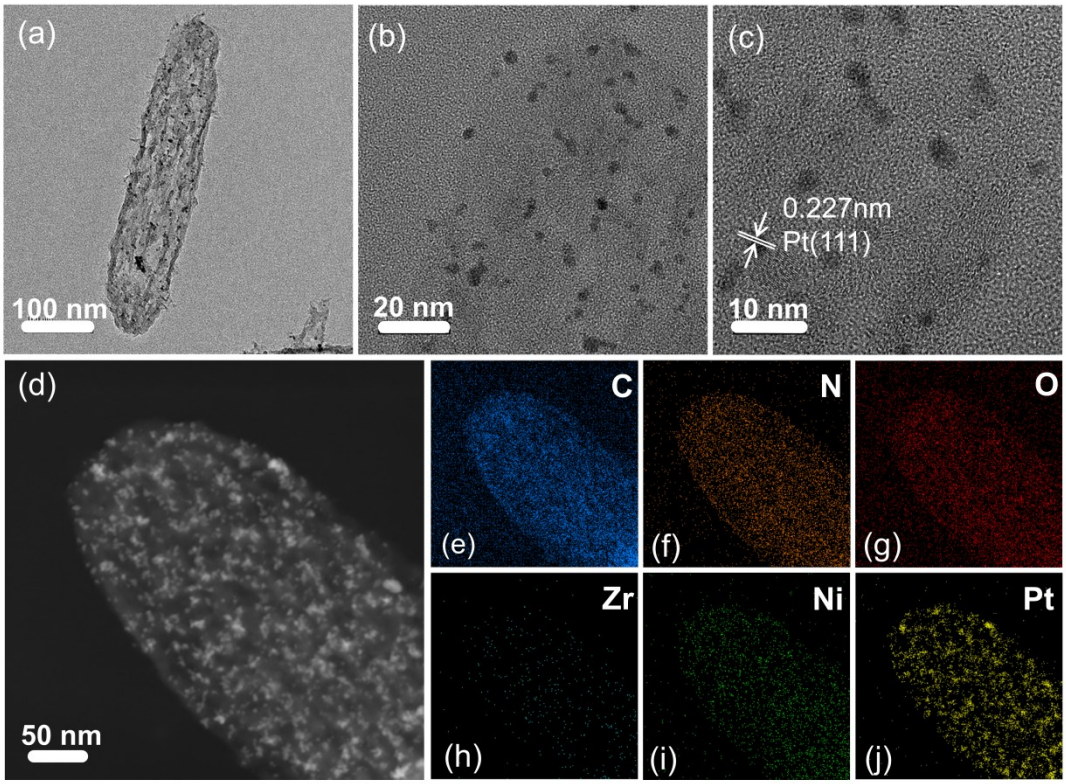


**Fig. S9.** (a, b) TEM, (c) HRTEM, (d) STEM images and (e-j) AC-STEM-EDS elemental mapping for $Pt_{10}/ZrO_2$-NC after CP for 230 h.

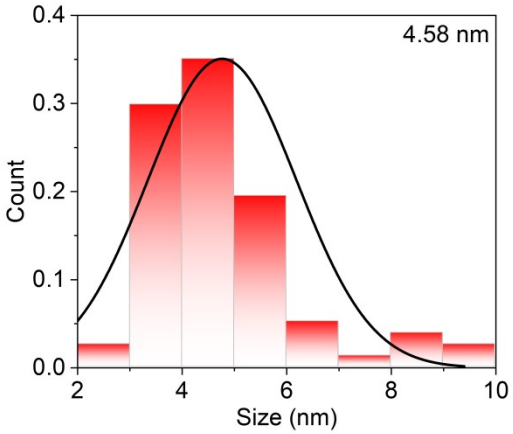


**Fig. S10.** Particle size distribution of $Pt_{10}/Ni\text{-}ZrO_2$-NC after CP for 230 h.

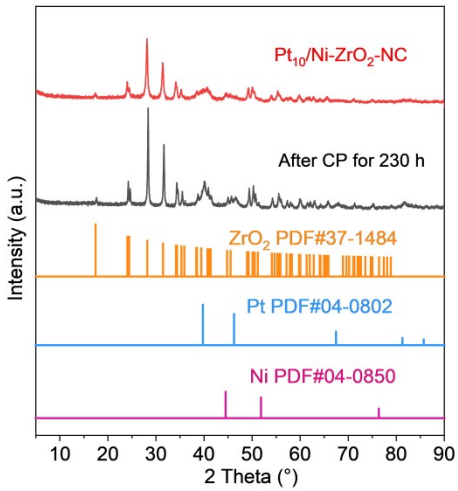


**Fig. S11.** XRD patterns of $Pt_{10}$/Ni-$ZrO_2$-NC after CP for 230 h.

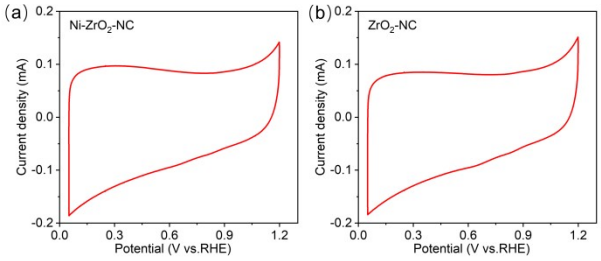


**Fig. S12.** Electrocatalytic performance toward the MOR (scan rate of 50 mV $s^{-1}$)

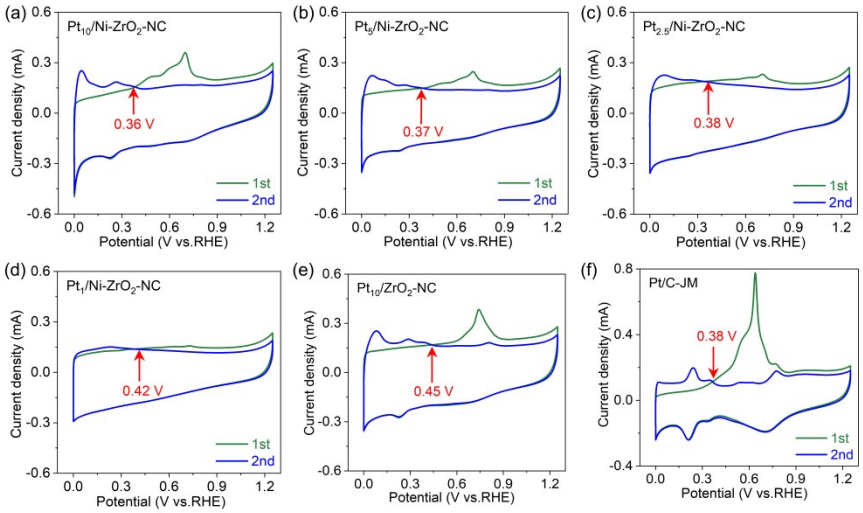


**Fig. S13.** CO stripping experiments for different catalysts.

Reference:

[1] N. Asano, S. Uemura, T. Kinugawa, H. Akasaka, T. Mizutani. J. Org. Chem., 2007, **72,** 5320-5326.